

# Influence of geometry on mechanical properties of bio-inspired silica-based hierarchical materials

Leon S Dimas and Markus J Buehler<sup>1</sup>

Department of Civil and Environmental Engineering, Laboratory for Atomistic and Molecular Mechanics (LAMM), Massachusetts Institute of Technology, 77 Massachusetts Ave., Cambridge, MA 02139, USA

E-mail: [mbuehler@MIT.EDU](mailto:mbuehler@MIT.EDU)

Received 27 March 2012


Accepted for publication 1 June 2012

Published 28 June 2012

Online at [stacks.iop.org/BB/7/036024](http://stacks.iop.org/BB/7/036024)

## Abstract

Diatoms, bone, nacre and deep-sea sponges are mineralized natural structures found abundantly in nature. They exhibit mechanical properties on par with advanced engineering materials, yet their fundamental building blocks are brittle and weak. An intriguing characteristic of these structures is their heterogeneous distribution of mechanical properties. Specifically, diatoms exhibit nanoscale porosity in specific geometrical configurations to create regions with distinct stress strain responses, notably based on a single and simple building block, silica. The study reported here, using models derived from first principles based full atomistic studies with the ReaxFF reactive force field, focuses on the mechanics and deformation mechanisms of silica-based nanocomposites inspired by mineralized structures. We examine single edged notched tensile specimens and analyze stress and strain fields under varied sample size in order to gain fundamental insights into the deformation mechanisms of structures with distinct ordered arrangements of soft and stiff phases. We find that hierarchical arrangements of silica nanostructures markedly change the stress and strain transfer in the samples. The combined action of strain transfer in the deformable phase, and stress transfer in the strong phase, acts synergistically to reduce the intensity of stress concentrations around a crack tip, and renders the resulting composites less sensitive to the presence of flaws, for certain geometrical configurations it even leads to stable crack propagation. A systematic study allows us to identify composite structures with superior fracture mechanical properties relative to their constituents, akin to many natural biomineralized materials that turn the weaknesses of building blocks into a strength of the overall system.

 Online supplementary data available from [stacks.iop.org/BB/7/036024/mmedia](http://stacks.iop.org/BB/7/036024/mmedia)

(Some figures may appear in colour only in the online journal)

## 1. Introduction

The study of the mechanics of mineralized biological structures has emerged as an important area of research with potential implications for bio-inspired materials design. Experimentally, these structures have been shown to exhibit high elastic moduli of several hundred GPa, great strengths and fracture toughness as large as  $8 \text{ MPa m}^{1/2}$  (e.g. for nacre), far

exceeding that of their building blocks alone [1–10]. Several earlier studies have focused on studying these properties in light of their hierarchical nature [11–16]. With the advancement of computational tools, *in silica* studies have also become a popular tool used to gain fundamental insight into the design principles employed by nature in developing advanced materials from primitive building blocks [17–22]. In [17] it was shown that the nanometer size of certain structural features in mineralized structures might be selected to optimize local flaw tolerance. In [19] the authors argue that mineralized structures

<sup>1</sup> Author to whom any correspondence should be addressed.

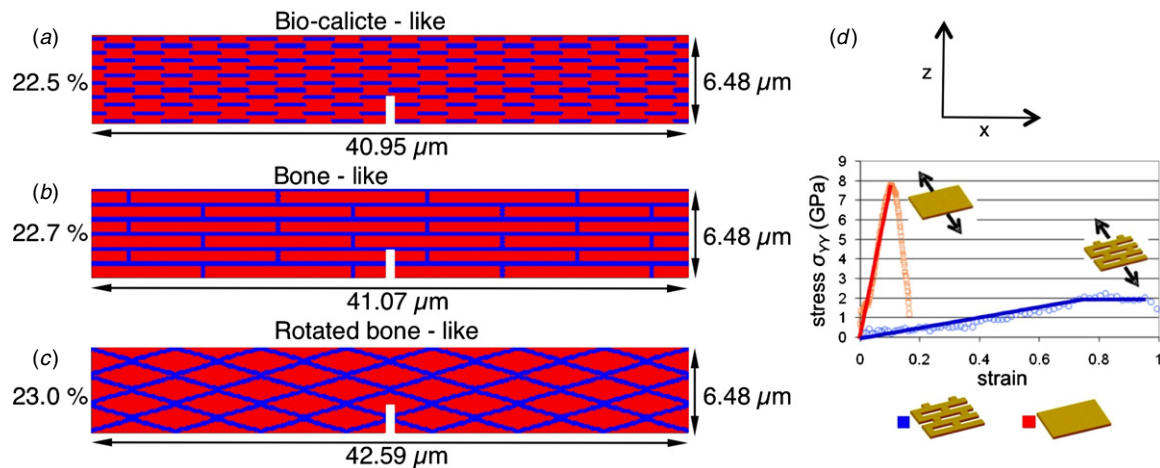


**Figure 1.** Geometries of specimens, here shown with size parameter  $h = 6.48 \mu\text{m}$ . With the darker (blue) and lighter (red) phases representing the nanoporous and bulk silica, respectively, for (a) the bio-calcite-like geometry, (b) the bone-like geometry and (c) the rotated bone-like geometry. The specimens are loaded by imposing stepwise displacement on their right vertical faces, whilst holding the left hand sides still. Periodic boundary conditions are employed in the horizontal direction. (d) Constitutive laws for the nanoporous and bulk silica phase representing the compliant and brittle phase respectively in our material model (adapted from [21] with permission from Nature Publishing Group).

with staggered arrangements of mineral platelets, such as nacre and bone, can attribute their impressive fracture toughness's to the energy dissipation mechanisms of the proteinaceous layers in between the mineral platelets. In [21] it was shown in a diatom inspired system that adding more levels of hierarchies significantly increases the toughening behavior of silica-based mineralized structures.

The key contribution of this paper is the elucidation of design principles for mineralized structures at a very fundamental level. We emphasize that we do not intend to model specific biological species or materials. Rather we draw inspiration from a range of biological mineralized structures to build model materials and assess generic design principles. We specifically look beyond complex and highly species-specific structural features such as proteinaceous layers and focus on the simplest principles that we believe make key contributions to the fundamental mechanical response of these structures. At some level, diatoms, bone, nacre and deep-sea sponges universally consist of more and less compliant regions arranged in specific geometries. We hypothesize that ordering these softer and stiffer regions in specific geometrical arrangements is a powerful design principle for creating functional materials from inferior building blocks. In fact, in light of this principle we expect that tuning and optimizing a confined number of simple geometric features of a single brittle material, e.g. silica, can produce superior materials. In this study we show that the inclusion of a deformable nanoconfined silica phase in bulk silica structures can be sufficient if introduced and distributed in an appropriate manner. By studying the mechanisms of deformation and failure of model materials we investigate the detailed mechanisms by which deformable and brittle regions interact to form a fracture resistant composite, and which details of their structural configuration make their interaction advantageous for meso- and macroscale structures. Finally we argue that the compliance of the second phase is the key

attribute enhancing the overall mechanical behavior of the composite and the specific mechanisms by which the response is enhanced depends on the geometrical configuration of the deformable phase.

Inspired by mineralized structures, e.g. the frustules of diatom algae, bone, nacre and deep-sea sponges, we direct our focus toward the mechanics of materials consisting of regions with distinct constitutive behavior arranged in several distinct yet intelligible patterns. Our material system consists purely of silica and the constitutive laws of the different regions differ by their compliance and failure strains. We emphasize the interactions between these regions and attribute mechanisms of deformation and failure to their distinct arrangements. We believe that by choosing silica as the sole building block of our systems we can demonstrate a greater level of generality of our results. Figure 1 pictures the geometries chosen for investigation, (a) a bio-calcite-like geometry, (b) a bone-like geometry and (c) a rotated bone-like geometry. The two first geometries are examined for their simplicity and contrasting nature. The bio-calcite-like comprising of soft platelets dispersed in a stiff matrix and the bone-like consisting of stiff platelets staggered in a compliant matrix. These differences are hypothesized to define the fundamental mechanics of the structures, changing methods of longitudinal and shear, stress and strain transfer and thus have large implications on sensitivities to cracks and size dependences of strength. The third, rotated bone-like, geometry is included in an attempt to optimize strain transfer through the structures. By providing a continuous path for longitudinal strain transfer, we hypothesize that one can induce ductility of the structure and eliminate the catastrophic nature of failure commonly associated with silica.

## 2. Materials and methods

The models analyzed here are based on a multiscale bottom-up computational approach, they consist purely of silica, in

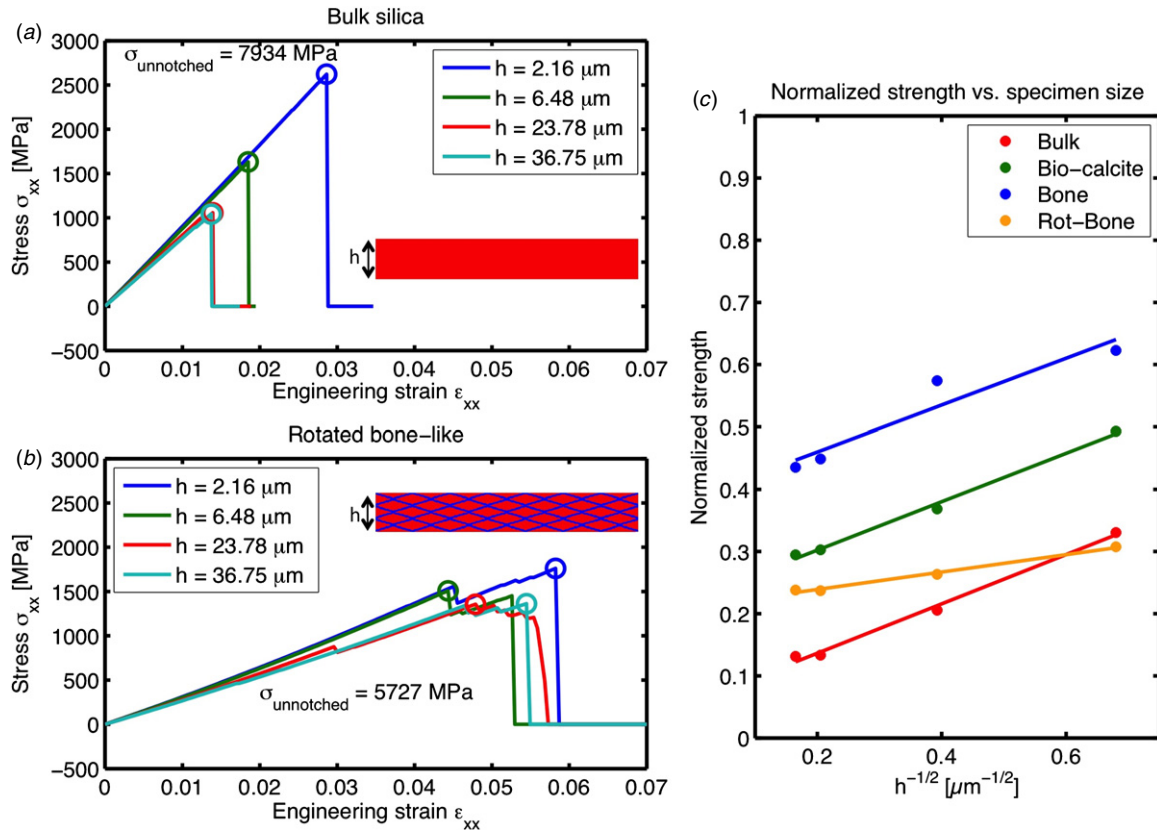


**Figure 2.** (a) Stress versus strain response for the bulk silica specimen, and (b) the rotated bone-like specimen. Circular markers indicate the points at which the ultimate stress snapshots are taken. The strain measure employed here is a macroscale measure of strain and is measured as the change in length normalized by the initial unstressed length (c). Normalized strength as a function of specimen size for all three considered geometries as well as the bulk silica sample. The strengths are normalized with respect to the respective strengths of the unnotched samples. It is clearly seen that both the bio-calcite-like geometry and bone-like geometry retain significantly larger portions of their unnotched strength under the influence of the flaw thus exhibiting more robust and desirable behavior. For example, whereas the notched  $6.48 \mu\text{m}$  bulk silica specimen attains a mere 20% of its unnotched strength the bone-like structure fails at almost 60% of its unnotched strength.

bulk and nanoporous form exhibiting fundamentally different constitutive behavior as shown in figure 1(d). The load deformation behavior of the two phases constituting our model is characterized by full atomistic studies with the first principles based ReaxFF force field. These stress-strain behaviors are used to coarse-grain the material in order to run simulations at meso- and macro-length scales. Such coarse-graining for computational studies of fracture in heterogeneous materials has been validated in several independent studies [23–25]. The employed material model has been developed and studied in previous work, where details on its formulation can be found [21, 22]. Here we apply the same model, employ it to a new geometry and report an in-depth analysis of the fundamental mechanical behavior.

The mechanical characteristics of the geometries are tested by introducing initial cracks at midsection extending through a fourth of the height of the specimens, constant notch length to sample size ratio and loading them until failure. To investigate size dependences, crack sensitivities and the up scaling of strength four different size parameters for the specimens are chosen:  $2.16$ ,  $6.48$ ,  $23.78$  and  $36.75 \mu\text{m}$ . The lengths of the specimens and their volume fractions of the soft phase are indicated in figure 1. The geometries were

created such as to keep these parameters as similar as possible and the inescapable disparities present are viewed as within an acceptable bound such that the geometries and results are comparable. The mechanical behavior of the composites is a function of the volume fraction of the soft phase. Increasing the volume fraction of the soft phase renders the composite more similar to nanoporous silica while decreasing the volume fraction of the soft phase makes the composite more similar to bulk silica. We choose a target volume fraction of around 20%. The goal is to create a composite that can combine the attractive mechanical features of its constituents. Thus our aim is to design a composite with appreciable stiffness, strength and fracture resistance and we choose a constant volume fraction to satisfy these requirements. It is noted that we have not sought to optimize the combination of these properties in terms of the volume fraction of the soft phase, but rather found a volume fraction that satisfies our requirements.

The loading is introduced by applying a displacement boundary condition on the right vertical face and holding the left vertical face fixed. After each displacement increment, the equilibrium positions of the beads are found by means of a conjugate gradient energy minimization technique. Hence, static loading is simulated. To avoid longitudinal size effects,

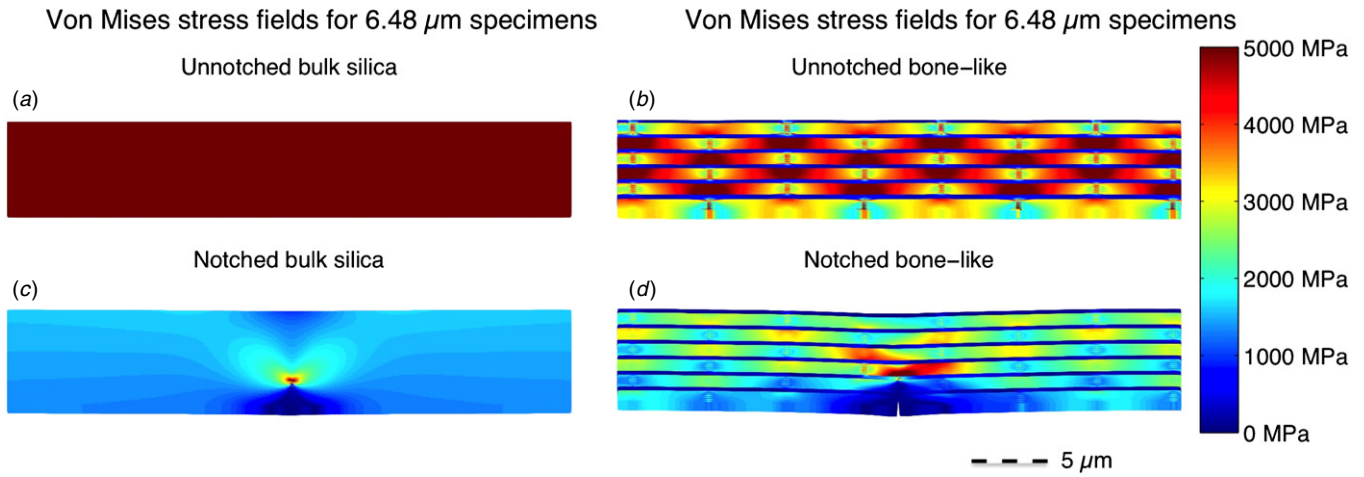


**Figure 3.** Von Mises stress fields for 6.48  $\mu\text{m}$  (a) unnotched bulk silica, (b) unnotched bone-like, (c) notched bulk silica and (d) notched bone-like specimens at the instant immediately prior to failure. The unnotched bulk silica specimen shows the expected even distribution of stress throughout the sample while the notched specimen exhibits the strong characteristic stress concentration at the crack tip. The unnotched bone-like specimen exhibits a clearly larger stress state than the notched specimen. However, the load path in both specimens is seen to be very similar. This specific hierarchical geometry alleviates the stress tip concentration and maintains the same mechanism of load transfer despite the presence of the crack, thus reducing the specimen's sensitivity to the notch.

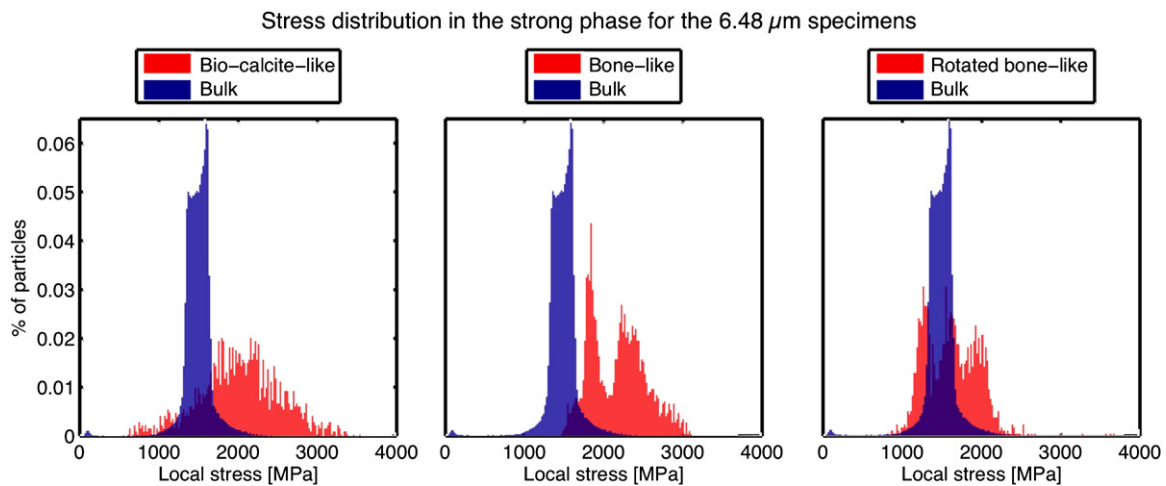


**Figure 4.** Plots comparing the stress distribution in the notched bulk geometry with the stress distribution within the strong particles of the (a) notched bio-calcite-like geometry, (b) the notched bone-like geometry and (c) the notched rotated bone-like geometry for the 6.48  $\mu\text{m}$  specimens. The plot clearly shows how the strong particles in the bio-calcite-like geometry and the bone-like geometry are significantly higher stressed than their counterparts in the bulk-silica specimen, thereby supporting the claim that the stronger phase in these structures is more efficiently utilized after the introduction of the notch than in their bulk silica counterpart.

periodic boundary conditions are employed in the  $x$ -direction. Stress and strain data are calculated at each displacement increment by recording positions of the beads throughout the deformation.

The stress measure used in this study is the virial stress [26]. For the study of local deformations the Zimmerman virial deformation measure [27] is applied. The computed local stresses and strains are evaluated by visualization of stress and strain fields plotted in MATLAB. Stress and strain fields represent an important analysis tool in this study as they provide insight into the modes of deformation and failure of the materials. These field plots can also provide insight to the role of the soft phase and its geometrical configuration in the context of strain and stress transfer. It should be

noted that strains in the immediate vicinity of the crack tip might be inaccurate due to the inhomogeneity of deformation fields in this region. However, we argue that the toughening mechanisms are mainly encountered away from the crack tip and hence the strain plots are meaningful.

Before we start discussing our results we point out a few important points. We recognize and appreciate the large range and great complexity of deformation mechanisms that occur throughout the loading of mineralized structures, as has been studied by several groups [7, 9, 11, 13, 15]. Our goal in the present analysis is not to capture all of these mechanisms, and thus our models are not designed to incorporate them all. Rather, we are specifically interested in how the interplay of soft and stiff regions organized in specific arrangements



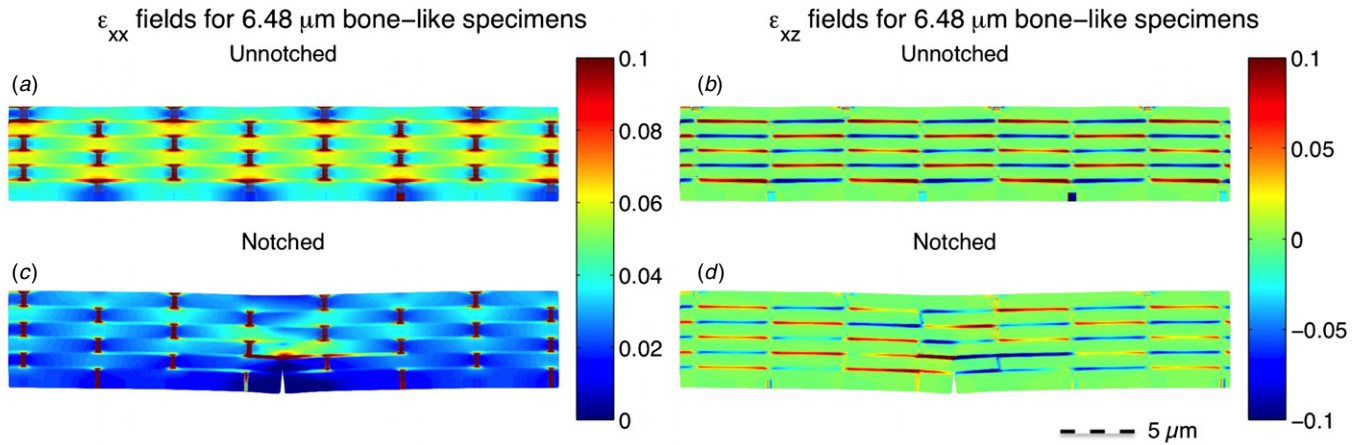


**Figure 5.** (a) Longitudinal and (b) shear strain fields for unnotched bone-like geometry at the instant immediately prior to failure. (c) Longitudinal and (d) shear strain fields for notched bone-like geometry at the instant immediately prior to failure. Whereas the longitudinal strain transfer is significantly impeded in the stiff phase by the introduction of the crack the panels clearly show that the strain field in the soft compliant phase remains virtually unchanged.

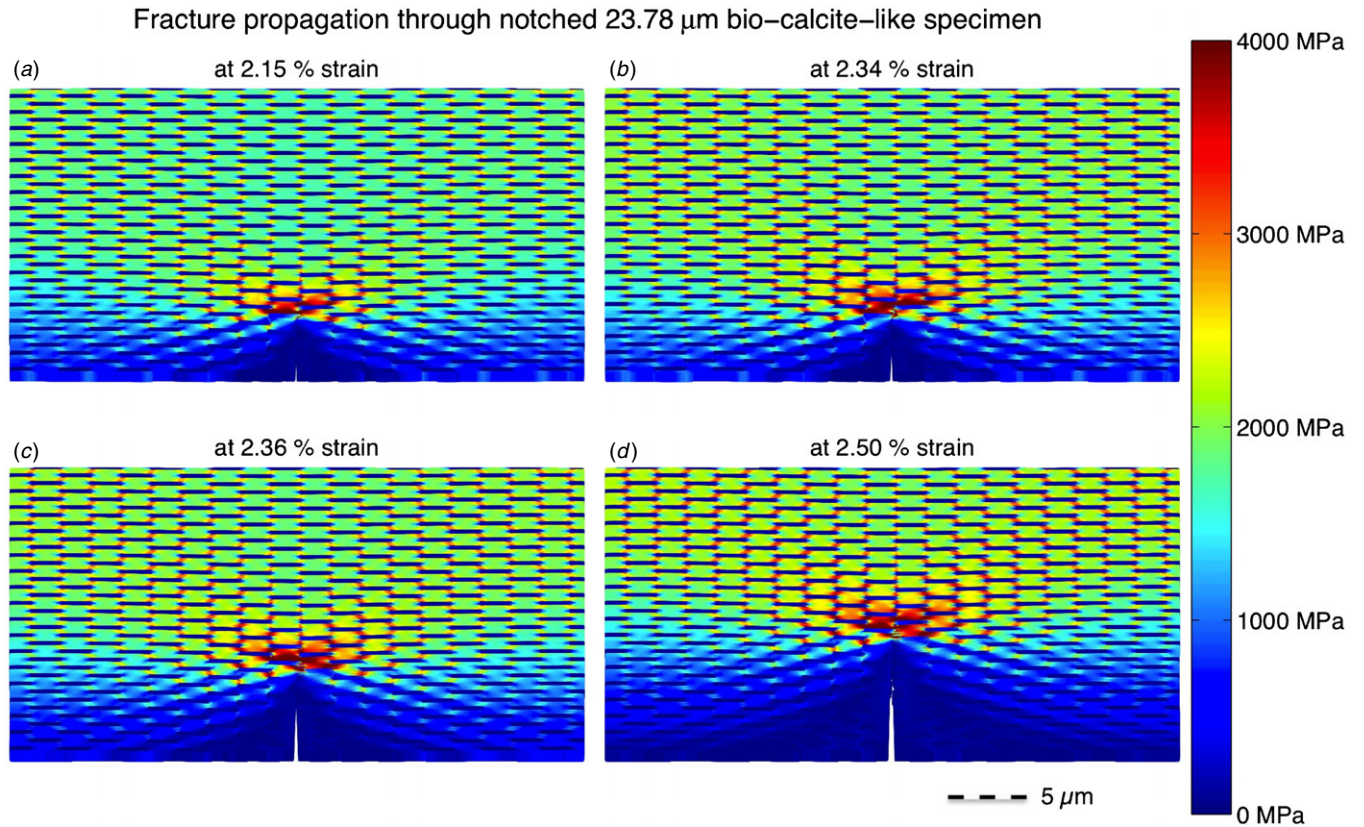


**Figure 6.** Crack propagation through 23.78  $\mu\text{m}$  bio-calcite-like specimen. Snapshots taken at (a) 2.15% strain, (b) 2.34% strain and maximum loading, (c) 2.36% strain and (d) 2.50% strain and immediately prior to complete failure of the specimen. Strain increments are 0.017% strain between the panels. To visualize details in the distribution of stresses the maximum limit of the color bar was lowered to 4000 MPa.

affects the structural response of a composite. We wish to observe mechanisms induced solely by these interactions and isolate them through our specific model design. This choice means that failure in our model materials cannot be directly translated to failure in natural mineralized structures. However, we believe that the observed mechanisms can provide a deeper insight into the natural mechanisms by isolating them in our models.

### 3. Results and discussion

The contrasting macroscopic stress–strain response of the bulk silica samples and the rotated bone-like geometry samples is illustrated in figures 2(a) and (b). Figure 2(c) shows the normalized strength plotted versus the inverse square root of the size parameter of the specimens for all specimens tested. The stresses are normalized by the ultimate stresses

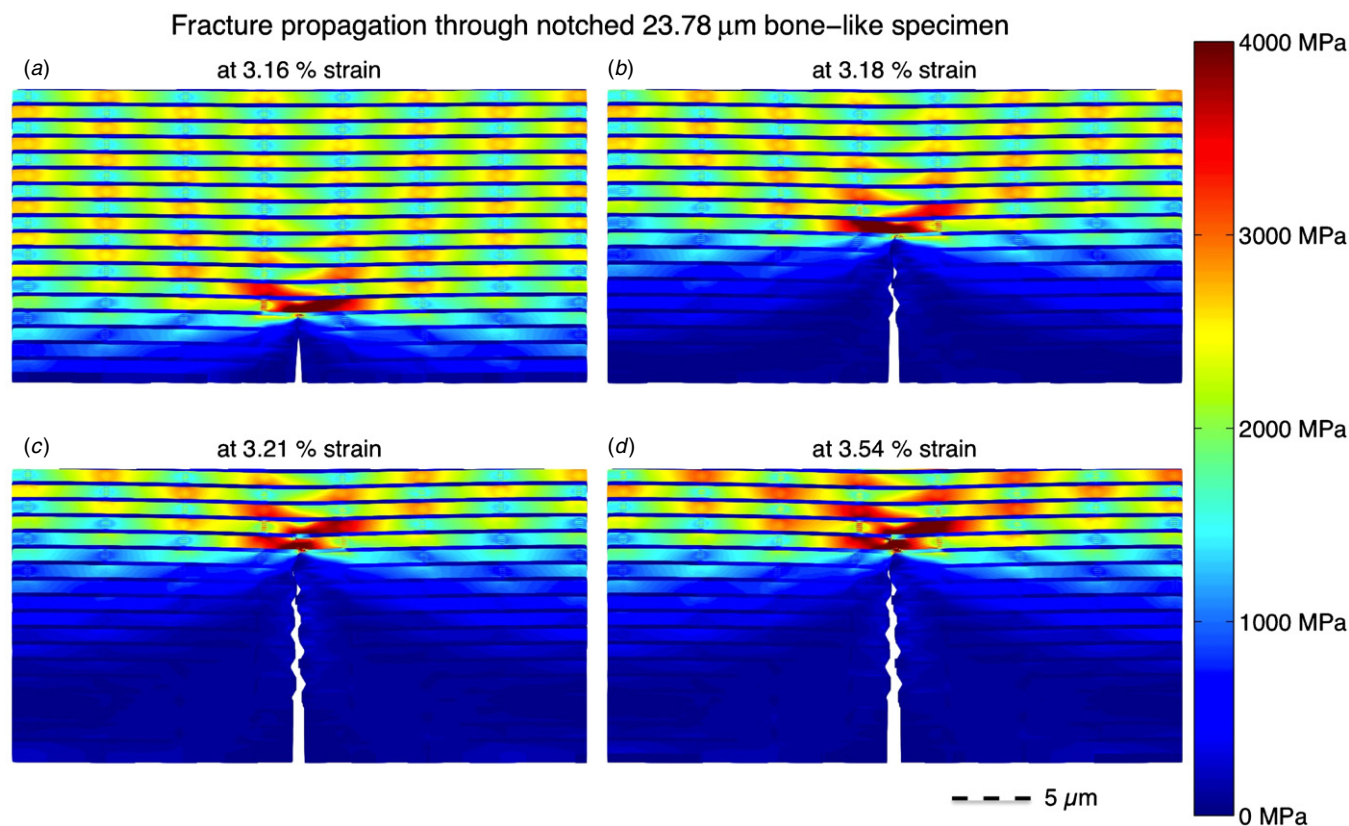


**Figure 7.** Crack propagation through 23.78  $\mu\text{m}$  bone-like specimen. Snapshots taken at (a) 3.16% strain and maximum loading, (b) 3.18% strain, (c) 3.21% strain and (d) 3.54% strain and immediately prior to complete failure of the specimen. Strain increments are 0.019% strain between the panels. (c) and (d) both correspond to states where the stress in the sample has dropped to half of its peak value and at this point the specimen has effectively failed. To visualize details in the distribution of stresses the maximum limit of the color bar was lowered to 4000 MPa.

for the respective unnotched specimens. Comparing the stress strain responses of the bulk-silica and the rotated bone-like geometry it is seen that the failure mechanism has transitioned from a catastrophic immediate failure for the bulk silica samples to a ductile more stable fracture for the rotated bone-like geometry. Also, in strong contrast to the bulk silica specimens, the strength of the notched rotated bone-like specimens is seen to be practically independent of size. Further considering figure 2(c), the strengths of both the bio-calcite-like and bone-like geometry show a significantly lesser sensitivity to the presence of the crack. Figure 2, complemented by the remaining stress-strain responses presented in the supplementary material available at [stacks.iop.org/BB/7/036024/mmedia](http://stacks.iop.org/BB/7/036024/mmedia), show that the composites maintain appreciable stiffness and strength with the humble volume fraction of compliant nanoporous silica chosen. In order to gain a more fundamental understanding of the mechanisms controlling the responses exemplified in figure 2, stress and strain field plots are investigated.

### 3.1. Ordered arrangement of nanoporous silica—decreasing strength sensitivity to cracks

Figure 3 shows the Von Mises stress fields immediately prior to failure for the unnotched and notched specimens of the

6.48  $\mu\text{m}$  bulk silica and bone-like geometry. The panels clearly illustrate the reduced crack sensitivity exhibited by the hierarchical bone-like geometry. Whereas the load transfer in bulk silica specimens is highly reactive to the presence of the crack, the bone-like geometry is significantly less affected. The Von Mises stress field for the bulk silica sample goes from one where the stress is uniformly distributed throughout the sample to a situation where the stress is highly concentrated in the immediate vicinity of the crack tip. The bulk of the material is virtually unstressed as opposed to the unnotched case and the stress field has completely changed as a result of the introduction of the crack. The bone-like geometry exhibits contrasting behavior. Still, the stress level drops by introduction of the notch, however inspection and comparison of figures 3(b) and (d) shows that the overall method of stress transfer is the same. The stress distribution is far less affected by the crack and the stress concentration at the crack tip is significantly less prevalent. The soft matrix renders a far less sensitive response to the notch for the overall structure and a more efficient material usage, the bar plot depicted in figure 4(b) clearly illustrates this point. Figure 4 illustrates, for all notched geometries tested of 6.48  $\mu\text{m}$  size, the efficiency of material usage in an intelligible manner. It depicts the distribution of stress levels felt by the stiffer particles. Interpreting the mean of these stress levels as a measure of efficiency of material usage it is seen that both



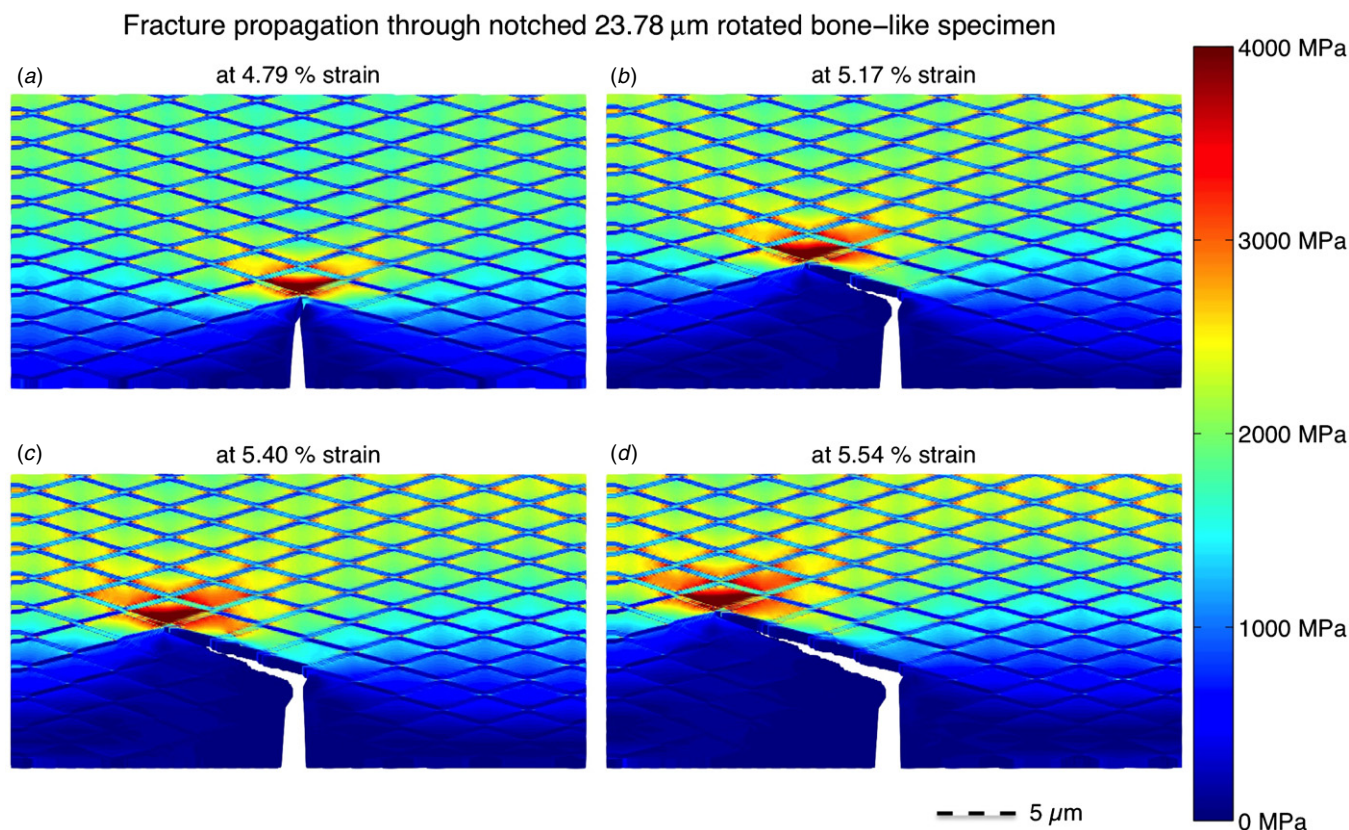


**Figure 8.** Stable crack propagation through 23.78  $\mu\text{m}$  rotated bone-like specimen. Snapshots taken at (a) 4.79% strain, (b) 5.17% strain, (c) 5.40% strain and (d) 5.54% strain and immediately prior to unstable crack propagation. Strain increments are 0.047% strain. To visualize details in the distribution of stresses the maximum limit of the color bar was lowered to 4000 MPa.

the bio-calcite-like and bone-like geometry far outperform the bulk silica specimen in this sense.

Referring to figure 2(c) the 6.48  $\mu\text{m}$  notched sample of the bone-like geometry is seen to reach a strength almost 60% that of its unnotched counterpart, quite impressive as opposed to the notched bulk silica sample which endures less than 20% of its theoretical strength. In this context we note that the vertical parts of the soft continuous phase in the bone-like geometry actually carry a significant stress, despite their compliance and weakness! This likely has an effect on the crack sensitivity of the geometry and when discussing crack sensitivity we are essentially also discussing the flaw tolerant size. A structure with a large flaw tolerant size is less sensitive to cracks at larger length scales than a structure with a very small flaw tolerant size. Regarding the tested specimens in this study as single edged notched tensile specimens, conventional linear elastic fracture mechanics predicts the flaw tolerant size to scale with the inverse square root of the strength of the material [28]. The specific geometrical configuration of the soft phase in the bone-like geometry thus increases the flaw tolerant size of the material for this loading condition by transferring significant stresses through the weak phase.

Despite this effect we appreciate that the compliance of the soft phase makes it most appropriate for absorbing deformation. Therefore, its role in reducing the bone-like specimens' sensitivity to the crack is best understood by inspection and comparison of the strain fields for the unnotched

and notched specimen of the bone-like geometry, as shown in figure 5. (The strain fields for the bulk silica specimens are easily inferred from the stress fields and thus not presented here.) Whereas the notch effectively reduces the spreading of longitudinal strain in the stiff phase, the compliance of the weaker phase allows this phase to maintain a state of large longitudinal strain despite the notch. Further, as the shear strain transfer occurs almost exclusively through the continuous nanoporous silica phase the shear strain fields for the uncracked and cracked specimens are close to identical. Strain will naturally tend to concentrate in regions of least resistance. In very strong and rigid structures such regions are commonly represented by cracks, where localizations of strains and stresses lead to sudden catastrophic failures, as exemplified by the notched bulk silica. Introducing a compliant weaker phase provides alternate regions for the strain to concentrate in and around. When appropriately arranged the softer phase is here shown to be able to make the effect of the crack less critical by employing its compliant nature as to absorb significant strains away from the crack tip thereby more evenly distributing stresses throughout the sample and thus minimizing the effect of the notch. The specimen to some extent 'forgets' that it has a crack and strains and stresses flow in similar ways as in the unnotched case. The geometrical configuration of the soft matrix decreases the sensitivity to the crack by means of its compliance and architecture.

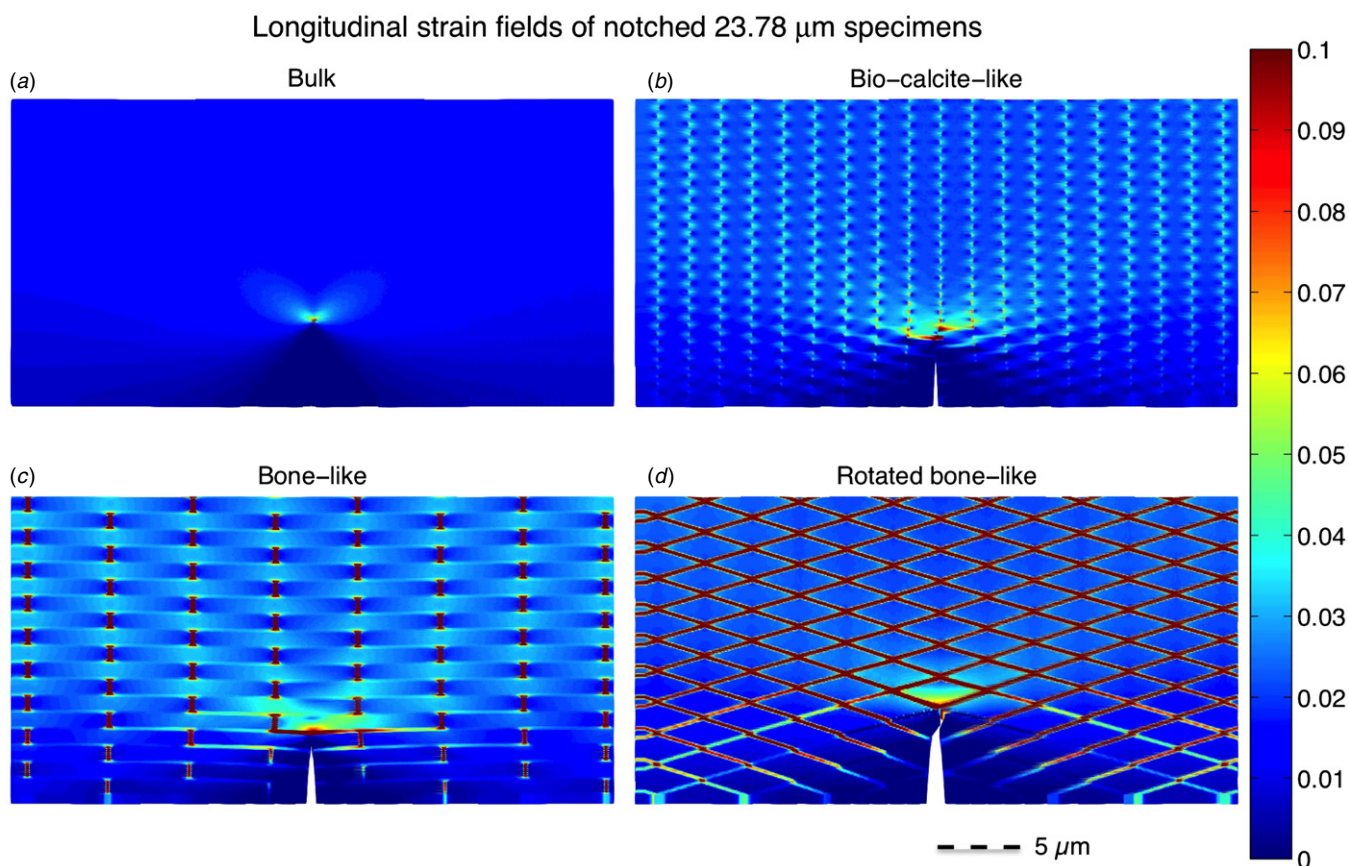


**Figure 9.** Longitudinal strain fields for 23.78  $\mu\text{m}$  (a) bulk-silica, (b) bio-calcite-like, (c) bone-like and (d) rotated bone-like notched specimens at the instant where each of the specimens reach their maximum loading. The plots illustrate how the distribution of the soft phases controls the pattern of the strain transfer, and thereby enables a distinct mechanism of deformation and failure.

### 3.2. Introduction of weak links—stabilizing fracture

Failure and fracture of brittle materials such as silica and also silicon is well studied [29, 30]. Upon loading such materials build up large stress concentrations around flaws and crack tips. When these stress concentrations reach some critical value the cracks propagate catastrophically at very large speeds leading to complete failure of the materials. Such catastrophic fracture commonly occurs without warning and thus these types of failure are not ideal. Figures 6 through 8 illustrate the propagation of fracture through our tested samples with constant size of 23.78  $\mu\text{m}$ . The cracks propagate rapidly without large increments in strain for both the bio-calcite-like geometry in figure 6 as well as for the bone-like geometry in figure 7. The potential for sustaining loading also drops quickly as fracture progresses in these geometries. However, the rotated bone-like geometry shows a quite contrasting behavior. The visualizations of the fracture propagation provided in figures 8(a)–(d) show desirable stable crack propagation through the specimen. The titles of the individual panels indicate the strain state at which the snapshots are taken: 4.79%, 5.17%, 5.40% and 5.54%, respectively. The strain increment at each step of the simulation for this particular geometry is 0.047%. Fracture occurs gradually and stably, significant increasing deformations can be sustained and the specimen endures a high level of stress despite the propagating crack. Inspect these panels in connection with figure 2(b), the

fracture propagation corresponds to the yielding plateau of the stress–strain response. The key here is the inclination of the soft phase. The inclination allows the longitudinal strains to flow continuously throughout the specimens, as opposed to the other inspected geometries, see figure 9, thus enabling the crack to be entrapped in the soft phase. Consequently, the crack tip is blunted and as stress concentrations scale with the inverse square root of the crack tip radius the severity of the crack lessens and a stable propagation of fracture is achieved. The ordered geometry of the nanoporous silica phase introduces significant toughening mechanisms in a composite with silica as its building block, a material commonly known as very brittle.

### 3.3. Comparing strain transfer in 23.78 $\mu\text{m}$ specimens—summarizing findings

Figure 9 ties together the discussion above. It presents strain field plots at the instant the geometries endure their greatest loading for all 23.78  $\mu\text{m}$  specimens studied. Figure 9(a) shows the large concentrations of strains in the bulk silica configuration, the strain distribution we aimed to distance our structures from by introducing the compliant phase in ordered arrangements. Figures 9(b) through (d) present the more evenly distributed and desirable strain fields observed for the composite structures. The soft phases present new areas where strains tend to develop, thus forcing strains to distribute



in accordance with its arrangement and delocalizing loading from the crack.

Comparing the behaviors in figures 9(b)–(d) the large influence of the specific geometries is apparent. We observe that the strain transfer in the bio-calcite like geometry in figure 9(b) is obstructed by poor communication of strain through the stiff matrix. However, the geometries with a continuous soft phase in figures 9(c) and (d) show a superior strain distribution and higher strain levels despite constituting of the same building blocks. Further, the large longitudinal strain achieved in the vertical compliant phase of the bone-like geometry actively employs the stiff platelets in the transfer of strain thereby giving the structure a robust response independently of the presence of the flaw. Finally, the inclined nature of the deformable phase in the rotated bone-like geometry allows the longitudinal strain to flow continuously throughout the specimen. Flaws thereby become trapped within this phase, preventing catastrophic failure and stabilizing fracture.

### 3.4. Manufacturability of geometries and scalability of results

Much effort has been devoted to creating artificial mimics of mineralized structures with geometries similar to the composites discussed in our study [31–33]. One of the biggest challenges is the dominance of nanosized structural features characteristic of these materials. Despite many advances a large-scale cost-effective production method of such synthetic structures is still out of reach. An upswing of focus on self-assembly techniques as highlighted in [31] provides exciting outlooks. Despite the clear advantage of nanoscale structural features in terms of increased flaw tolerance we argue that our results could show that nature's design principles are applicable and useful at a range of length scales, length scales at which large-scale cost-effective production methods do exist. A spring bead model such as the one we have employed can be scaled up to larger length scales with the appropriate adjustment of constitutive relations for the springs. Further the employed constitutive relations are quite generic and neither are they limited to certain length scales. Thus we also expect our results can be exploited in larger scale applications, and are valid for geometries with features at length scales beyond the nanoscale.

## 4. Conclusion

The study reported here has investigated the mechanics and deformation mechanisms of mesoscale structures composed of phases with contrasting constitutive behavior ordered in specific configurations. By conducting this study with a simple model in a systematic manner, exploring the effect of different geometries and sizes and the effect of the presence of flaws we have gained a more fundamental insight into intelligible principles employed by nature in its design of mineralized materials. The mechanism by which a simple compliant phase can improve the mechanical behavior of a flawed structure at the mesoscale can desensitize a structure to a flaw simply by means of its soft nature. As opposed to a stiff and strong

material where stresses concentrate around flaws like cracks or voids, the soft phase in our composites provides an alternate route for deformation and the methods of strain transfer and mechanisms of failure depend on its geometrical distribution. A brick and mortar like distribution of the stiff and soft phase was shown to give a far more efficient material usage in the presence of a crack, while an inclined continuous soft phase was shown to inhibit catastrophic propagation of fracture. Further, showing that such attractive characteristics can be reached without a vast energy dissipation mechanism such as protein unfolding and without the addition of additional hierarchies exemplifies the importance of a detailed study of the particular design principles observed in nature. Only through such a study can we attain fundamental insights into these principles and gain a complete understanding of their potential. With the aim of optimizing synthetic material design and creating high performance materials at a low cost it is essential to exploit the full potential of every design principle employed, where the designs developed based on such paradigms encompass a merger of the concepts of structure and material [34] and could find widespread applications that range from architecture [35] to the design of innovative surfaces [36] or novel impact mitigating materials [37].

## Acknowledgment

Funding provided by DOD-Army Research Office (grant number W911NF1010127, program officer Larry C Russell).

## References

- [1] Almqvist N *et al* 2001 Micromechanical and structural properties of a pennate diatom investigated by atomic force microscopy *J. Microsc.* **202** 518–32
- [2] Hamm C E *et al* 2003 Architecture and material properties of diatom shells provide effective mechanical protection *Nature* **421** 841–3
- [3] Hildebrand M 2008 Diatoms, biomineralization processes, and genomics *Chem. Rev.* **108** 4855–74
- [4] Losic D, Mitchell J G and Voelcker N H 2009 Diatomaceous lessons in nanotechnology and advanced materials *Adv. Mater.* **21** 2947–58
- [5] Losic D *et al* 2007 Atomic force microscopy (AFM) characterisation of the porous silica nanostructure of two centric diatoms *J. Porous Mater.* **14** 61–9
- [6] Losic D *et al* 2007 AFM nanoindentations of diatom biosilica surfaces *Langmuir* **23** 5014–21
- [7] Weaver J C *et al* 2007 Hierarchical assembly of the siliceous skeletal lattice of the hexactinellid sponge *Euplectella aspergillum* *J. Struct. Biol.* **158** 93–106
- [8] Weaver J C *et al* 2003 Nanostructural features of demosponge biosilica *J. Struct. Biol.* **144** 271–81
- [9] Meyers M A *et al* 2008 Biological materials: structure and mechanical properties *Prog. Mater. Sci.* **53** 1–206
- [10] Barthelat F 2010 Nacre from mollusk shells: a model for high-performance structural materials *Bioinspir. Biomim.* **5** 035001
- [11] Aizenberg J *et al* 2005 Skeleton of *Euplectella* sp.: structural hierarchy from the nanoscale to the macroscale *Science* **309** 275–8
- [12] Miserez A *et al* 2008 Effects of laminate architecture on fracture resistance of sponge biosilica: lessons from nature *Adv. Funct. Mater.* **18** 1241–8

- [13] Weiner S and Wagner H D 1998 The material bone: structure mechanical function relations *Annu. Rev. Mater. Sci.* **28** 271–98
- [14] Peterlik H *et al* 2006 From brittle to ductile fracture of bone *Nature Mater.* **5** 52–5
- [15] Gupta H *et al* 2009 Nanoscale deformation mechanisms in bone *Bone* **44** S33–4
- [16] Buehler M J and Ackbarow T 2007 Fracture mechanics of protein materials *Mater. Today* **10** 46–58
- [17] Gao H J *et al* 2003 Materials become insensitive to flaws at nanoscale: lessons from nature *Proc. Natl Acad. Sci. USA* **100** 5597–600
- [18] Ji B H and Gao H J 2004 Mechanical properties of nanostructure of biological materials *J. Mech. Phys. Solids* **52** 1963–90
- [19] Ji B H and Gao H J 2004 A study of fracture mechanisms in biological nano-composites via the virtual internal bond model *Mater. Sci. Eng. A* **366** 96–103
- [20] Garcia A P, Pugno N and Buehler M J 2011 Superductile, wavy silica nanostructures inspired by diatom algae *Adv. Eng. Mater.* **13** B405–14
- [21] Sen D and Buehler M J 2011 Structural hierarchies define toughness and defect-tolerance despite simple and mechanically inferior brittle building blocks *Sci. Rep.* **1**
- [22] Sen D and Buehler M J 2010 Atomistically-informed mesoscale model of deformation and failure of bioinspired hierarchical silica nanocomposites *Int. J. Appl. Mech.* **2** 699–717
- [23] Curtin W A and Scher H 1990 Mechanics modeling using a spring network *J. Mater. Res.* **5** 554–62
- [24] Hassold G N and Srolovitz D J 1989 Brittle-fracture in materials with random defects *Phys. Rev. B* **39** 9273–81
- [25] Gao H J and Klein P 1998 Numerical simulation of crack growth in an isotropic solid with randomized internal cohesive bonds *J. Mech. Phys. Solids* **46** 187–218
- [26] Tsai D H 1979 Virial theorem and stress calculation in molecular-dynamics *J. Chem. Phys.* **70** 1375–82
- [27] Zimmerman J A, Bammann D J and Gao H J 2009 Deformation gradients for continuum mechanical analysis of atomistic simulations *Int. J. Solids Struct.* **46** 238–53
- [28] Tada H, Paris P C and Irwin G R 2000 *The Stress Analysis of Cracks Handbook* vol 20, 3rd edn (New York: ASME) p 677
- [29] Swadener J G, Baskes M I and Nastasi M 2002 Molecular dynamics simulation of brittle fracture in silicon *Phys. Rev. Lett.* **89** 085503
- [30] Buehler M J, van Duin A C and Goddard W A III 2006 Multiparadigm modeling of dynamical crack propagation in silicon using a reactive force field *Phys. Rev. Lett.* **96** 095505
- [31] Kroger N and Sandhage K H 2010 From diatom biomolecules to bioinspired syntheses of silica- and titania-based materials *MRS Bull.* **35** 122–6
- [32] Podsiadlo P *et al* 2007 Ultrastrong and stiff layered polymer nanocomposites *Science* **318** 80–3
- [33] Tang Z Y *et al* 2003 Nanostructured artificial nacre *Nature Mater.* **2** 413–8
- [34] Buehler M J and Yung Y C 2009 Deformation and failure of protein materials in physiologically extreme conditions and disease *Nature Mater.* **8** 175–88
- [35] Knippers J and Speck T 2012 Design and construction principles in nature and architecture *Bioinspir. Biomim.* **7** 015002
- [36] Lang A W *et al* 2008 Bristled shark skin: a microgeometry for boundary layer control? *Bioinspir. Biomim.* **3** 046005
- [37] Cranford S W *et al* 2012 Nonlinear material behaviour of spider silk yields robust webs *Nature* **482** 72